Journal of Applied Electrochemistry **31**: 93–98, 2001.
© 2001 *Kluwer Academic Publishers. Printed in the Netherlands.*

Calculation of the e.m.f. of solid oxide fuel cells

S.W. ZHA, C.R. XIA and G.Y. MENG*
Department of Materials Science and Engineering, University of Science and Technology of China, Hefei, 230026, China
*(*author for correspondence, e-mail: mgym@ustc.edu.cn)*

Received 12 January 2000; accepted in revised form 20 July 2000

Key words: defect chemistry, electromotive force, solid oxide fuel cells

Abstract

The electromotive force (e.m.f.) of a solid oxide fuel cell (SOFC) based on fluorite structure electrolyte is calculated by defect chemistry analysis. This is strongly influenced by the characteristic oxygen pressure, $P^*_{O_2}$, at which the ionic transference number of the electrolyte is 0.5. It is concluded that e.m.f. decreases with increasing temperature to that of a purely ionic electrolyte-based fuel cell. The low anodic oxygen partial pressure has a smaller influence on the SOFC based on an electrolyte with mixed conduction than on the one based on a purely ionic electrolyte.

1. Introduction

A solid oxide fuel cell (SOFC) is an all-solid-state energy conversion device that produces electricity directly from a gaseous fuel (e.g., hydrogen, methane) by electrochemical combination of fuel and oxidant gases (usually oxygen) across an ionic conducting ceramic [1]. The SOFC has been extensively researched in recent years for its unique characteristics of having all-solid-state cell components, along with high operating temperature (500–1000 °C) offering a number of attractive features. Presently, yttria stabilized ZrO_2 (YSZ) is used, almost exclusively, as the electrolyte which conducts oxygen-ions from cathode to anode. Other oxygen-ion conductors such as doped CeO_2, stabilized Bi_2O_3, and doped $LaGaO_3$ have also been developed as electrolytes for SOFCs for reduced temperature operation (500–800 °C), due to their higher oxygen-ion conductivity than YSZ [2–6]. In addition, a number of proton-conducting materials have also been studied [7–10] for use as SOFC electrolytes.

When fuel gas and oxygen are applied to the anode and the cathode separately, an electromotive force (e.m.f.) is produced due to the electrochemical potential gradient of oxygen between the two electrodes. The SOFC is therefore considered to be an oxygen concentration cell. Cell e.m.f. is often expressed by the Wagner Equation [11]:

$$E = \frac{1}{4F} \int_{\mu'_{O_2}}^{\mu''_{O_2}} t_{\text{ion}} d\mu_{O_2} \qquad (1)$$

where F is the faradaic constant, t_{ion} is the transference number of oxygen ions which is defined as the ratio of the ionic conductivity to the total conductivity, and μ''_{O_2} and μ'_{O_2} are the chemical potentials of oxygen on the anode and cathode side of the electrolyte, respectively. By applying

$$\mu_{O_2} = \mu^0_{O_2} + RT \ln\left(\frac{P_{O_2}}{P^0_{O_2}}\right) \qquad (2)$$

where O2 is considered an ideal gas, the following relationship is obtained in combination with Equation 1 [12]:

$$E = \frac{RT}{4F} \int_{P'_{O_2}}^{P''_{O_2}} t_{\text{ion}} d \ln P_{O_2} \qquad (3)$$

where R is the gas constant, T is the absolute temperature, and P''_{O_2} and P'_{O_2}, corresponding to the chemical potentials of oxygen μ''_{O_2} and μ'_{O_2}, are the oxygen partial pressures at anode and cathode. Assumption of local equilibrium implies that O_2 is in equilibrium with oxygen-ions and electrons throughout the solid electrolyte. Therefore, a local partial pressure of P_{O_2} is equivalent to the local chemical potential of oxygen, μ_{O_2}, according to Equation 2. This local equilibrium assumption is typically used for the mass transport of oxide [13].

The open circuit voltage (o.c.v.) mainly determined by the e.m.f. is considered to be one of the most important parameters in evaluating an operating fuel cell. However, little work [14, 15] has been reported on the calculation of the theoretical e.m.f. of SOFCs. The objective of the present work was to calculate the e.m.f. of an SOFC theoretically based on the analysis of the defect chemistry. For simplicity, a fluorite structure oxide with oxygen ion conduction, A_2O_3-doped MO_2, was selected as the electrolyte; P''_{O_2}, Pt (anode) $|MO_2–A_2O_3|$Pt (cathode), P'_{O_2}. Other fluorite structure electrolytes can also be analysed by a similar method. These results can also be applied to SOFCs based on other electrolytes with some modification.

2. Theory and analysis

2.1. *Defect chemistry*

Doped MO_2 oxides such as stabilized ZrO_2 exhibit oxygen-ion conduction by transfer of oxygen-ions via oxygen-ion vacancies. Moreover, electrical conduction can also occur through mobile electronic charge carriers. Electronic and ionic transference numbers may vary depending on the surrounding gaseous environment. The dependence of the defect structure on oxygen partial pressure is considered here for a general system $MO_2–A_2O_3$, assuming intrinsic defects in pure MO_2 are of the Schottky type. Kröger–Vink notation is used to describe the various defects.

Oxygen vacancies result from incorporation of A_2O_3 into MO_2 as described by the following equation:

$$\tfrac{1}{2}A_2O_3 = A'_M + \tfrac{1}{2}V_O^{\cdot\cdot} + \tfrac{3}{2}O_O^{\times} \tag{4}$$

The environment gas, also affects the oxygen vacancies, as well as the electrons:

$$O_O = \tfrac{1}{2}O_2(g) + V_O^{\cdot\cdot} + 2\ e' \tag{5}$$

The intrinsic Schottky equilibrium and electronic equilibrium may be expressed as

$$\text{nil} = V_M'''' + 2\ V_O^{\cdot\cdot} \tag{6}$$

$$\text{nil} = \dot{h} + e' \tag{7}$$

The electroneutrality condition is given as

$$n + 4[V_M''''] + [A'_M] = p + 2[V_O^{\cdot\cdot}] \tag{8}$$

where n and p are the concentrations of electrons and holes, respectively.

2.2. *Ion conductivity*

The total electrical conductivity, σ_t, of the fluorite oxide $MO_2–A_2O_3$ includes five components according to Equation 8. It is noted that the ionic conductivity due to the migration of cations and cation vacancies (i.e., dopants A'_M and host cation vacancies V_M'''') can be neglected in the expression for σ_t. The approximation is based on cation diffusivity experiments, which showed mobilities of several orders of magnitude lower than that of $V_O^{\cdot\cdot}$. Thus, the total electrical conductivity, σ_t, is expressed as

$$\sigma_t = \sigma_{ion} + \sigma_n + \sigma_p \tag{9}$$

where σ_{ion}, σ_n and σ_p are electrical conductivities of oxygen-ion, electron and hole, respectively. Remembering that, under SOFC working conditions, the oxygen partial pressure in the cathode is typically 1 atm (pure oxygen) or 0.21 atm (air). σ_p, which is the conductivity attributed to the electron hole concentration, can also be neglected due to its much lower mobility compared to σ_n at such low oxygen partial pressure. Then we have:

$$\sigma_t = \sigma_{ion} + \sigma_n = 2\ e[V_O^{\cdot\cdot}]u_v + enu_n \tag{10}$$

where u_v and u_n refer to the mobilities of oxygen-ion vacancies and electrons, respectively.

A schematic representation of the conductivity as a function of P_{O_2} is shown in Figure 1. This figure was obtained by the following derivation. At low values of P_{O_2}, the electroneutrality condition (Equation 8) is given as

$$n = 2[V_O^{\cdot\cdot}] \tag{11}$$

From Equations 5 and 11, the concentration of n can be deduced as

$$n = (2Kv)^{1/3}P_{O_2}^{-1/6} \tag{12}$$

where Kv is the equilibrium constant of Equation 5. Since the mobility of electrons is generally 10^4 to 10^8 times higher than the mobility of oxygen vacancies, even at elevated temperature [16] the fluorite oxide under low P_{O_2} condition is approximated to be a pure n-type semiconductor. That is to say, the ionic transference number t_{ion} tends to zero. Therefore, the conductivity for $MO_2–A_2O_3$ under low oxygen partial pressures is given by

$$\sigma_t = \sigma_n = enu_n = e(2Kv)^{1/3}u_nP_{O_2}^{-1/6} \tag{13}$$

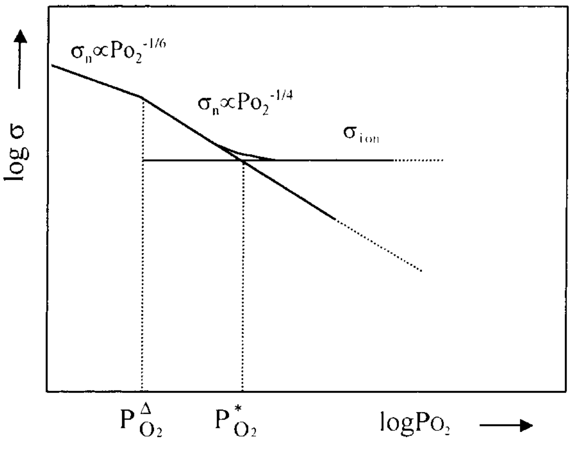

Fig. 1. Schematic illustration of the variation of electrical conductivity as a function of P_{O_2} for fluorite type oxide electrolyte.

At some intermediate oxygen partial pressures, in the range in which the two electrodes, especially the cathode of a practical SOFC, are operated, it is possible to approximate the electroneutrality condition of Equation 8 as

$$[\mathrm{A}'_{\mathrm{M}}] = 2[\mathrm{V}_{\mathrm{O}}^{\cdot\cdot}] \tag{14}$$

From Equations 5 and 14, the concentration of n can be deduced as

$$n = (2Kv/[\mathrm{A}'_{\mathrm{M}}])^{1/2} P_{\mathrm{O}_2}^{-1/4} \tag{15}$$

Thus, the total electrical conductivity can be expressed by

$$\sigma_{\mathrm{t}} = 2\,e[\mathrm{V}_{\mathrm{O}}^{\cdot\cdot}]u_{\mathrm{v}} + e(2Kv/[\mathrm{A}'_{\mathrm{M}}])^{1/2} P_{\mathrm{O}_2}^{-1/4} u_n \tag{16}$$

Although the above relationship $\sigma_n \propto P_{\mathrm{O}_2}^{-1/4}$ is obtained from theoretical analysis of defect chemistry, it is exactly in accordance with a number of experimental results of fluorite structure electrolytes such as doped $\mathrm{CeO_2}$ [17–19], doped $\mathrm{Bi_2O_3}$ [20, 21] and stabilized $\mathrm{ZrO_2}$ [22]. Now substituting Equation 16 into the defining expression for ionic transference number

$$t_{\mathrm{ion}} = \frac{\sigma_{\mathrm{ion}}}{\sigma_{\mathrm{t}}} \tag{17}$$

we obtain the following equation:

$$t_{\mathrm{ion}} = 2\,e[\mathrm{V}_{\mathrm{O}}^{\cdot\cdot}]u_{\mathrm{v}} / (2\,e[\mathrm{V}_{\mathrm{O}}^{\cdot\cdot}]u_{\mathrm{v}} + e(2Kv/[\mathrm{A}'_{\mathrm{M}}])^{1/2} P_{\mathrm{O}_2}^{-1/4} u_n) \tag{18}$$

For the sake of convenience, two specific oxygen partial pressures are marked as $P_{\mathrm{O}_2}^{\Delta}$ and $P_{\mathrm{O}_2}^{*}$ shown in Figure 1. $P_{\mathrm{O}_2}^{\Delta}$ represents the pressure at the transitional point of $\sigma_n \propto P_{\mathrm{O}_2}^{-1/6}$ and $\sigma_n \propto P_{\mathrm{O}_2}^{-1/4}$ · $P_{\mathrm{O}_2}^{*}$ corresponds to an oxygen partial pressure at which the ionic transference number becomes 0.5. The ionic conductivity at intermediate oxygen partial pressures can be assumed constant, because the doping of low valence atoms dominantly determines the concentration of oxygen-ion vacancies, compared to the defect reaction of Equation 5. Therefore, from the above definition of $P_{\mathrm{O}_2}^{*}$, the following equation is obtained based on Equation 18:

$$t_{\mathrm{ion}} = \frac{1}{1 + (P_{\mathrm{O}_2}/P_{\mathrm{O}_2}^{*})^{-1/4}} \tag{19}$$

2.3. *Calculation of the e.m.f.*

For an SOFC given as P''_{O_2}, Pt (anode) $|\mathrm{MO_2{-}A_2O_3}|$ Pt (cathode), P'_{O_2}, the e.m.f. can be given as follows after integration, and by substitution of t_{ion} into Equation 3:

$$E = \frac{RT}{F} \ln \frac{P_{\mathrm{O}_2}^{*1/4} + P_{\mathrm{O}_2}^{\prime 1/4}}{P_{\mathrm{O}_2}^{*1/4} + P_{\mathrm{O}_2}^{\prime\prime 1/4}} \tag{20}$$

when $P''_{\mathrm{O}_2} \geqslant P_{\mathrm{O}_2}^{\Delta}$, and

$$E = \frac{RT}{F} \ln \frac{P_{\mathrm{O}_2}^{*1/4} + P_{\mathrm{O}_2}^{\prime 1/4}}{P_{\mathrm{O}_2}^{*1/4} + P_{\mathrm{O}_2}^{\Delta 1/4}} \tag{21}$$

when $P''_{\mathrm{O}_2} < P_{\mathrm{O}_2}^{\Delta}$, since $t_{\mathrm{ion}} \rightarrow 0$ in the range $P_{\mathrm{O}_2} < P_{\mathrm{O}_2}^{\Delta}$. In the ideal case of a pure ionic electrolyte, $t_{\mathrm{ion}} = 1$, the e.m.f. can be derived directly from Equation 3 as

$$E = \frac{RT}{4F} \ln \frac{P'_{\mathrm{O}_2}}{P''_{\mathrm{O}_2}} \tag{22}$$

Equation 22 can be also obtained from Equation 20 by letting $P_{\mathrm{O}_2}^{*}$ become infinitely small, that is, $P''_{\mathrm{O}_2} \gg P_{\mathrm{O}_2}^{*}$.

3. Results and discussion

For the convenience of the following data analysis, a model of an SOFC based on fluorite structure electrolyte is assumed as P''_{O_2}, Pt (anode) |electrolyte| Pt (cathode), $P'_{\mathrm{O}_2} = 1$ atm [I]. The cathode is fed with pure oxygen as typically practised in a fuel cell. The anode is fed with $\mathrm{H_2O}$ moistened $\mathrm{H_2}$. Data for the variation of P_{O_2} with $\mathrm{H_2O}$ percentage in the mixture fuel gas (written as $\%\mathrm{H_2O{-}H_2}$) at different temperatures of 600, 800 and 1000 °C are shown in Figure 2 based on thermodynamic calculation. It can be seen that the oxygen partial pressures increase with increasing $\mathrm{H_2O}$ percentage in moisturized $\mathrm{H_2}$ and also with increasing temperature.

3.1. *Temperature effect on e.m.f.*

The temperature dependence of the e.m.f. of the above fuel cell [I] is given in Figure 3 when the electrolyte is a pure oxygen-ion conductor. The calculation is derived from Equation 22. The oxygen partial pressure, P''_{O_2}, at the anode is calculated by the thermodynamic equilibrium:

$$\mathrm{H_2(g)} + \tfrac{1}{2}\mathrm{O_2(g)} = \mathrm{H_2O(g)} \tag{23}$$

as

$$P''_{\mathrm{O}_2} = \left[\frac{P_{\mathrm{H_2O}}}{P_{\mathrm{H_2}}} \exp\left(\frac{\Delta G}{RT}\right)\right]^2 \tag{24}$$

where ΔG is the free energy change of Reaction 23 at temperature T(K), which can be calculated by using the Gibbs–Helmholtz equation. The influence of temperature on P''_{O_2} is exponential, which means the e.m.f. only depends on the working temperature when the anode is fed with a certain $\mathrm{H_2O{-}H_2}$ gas mixture. At different

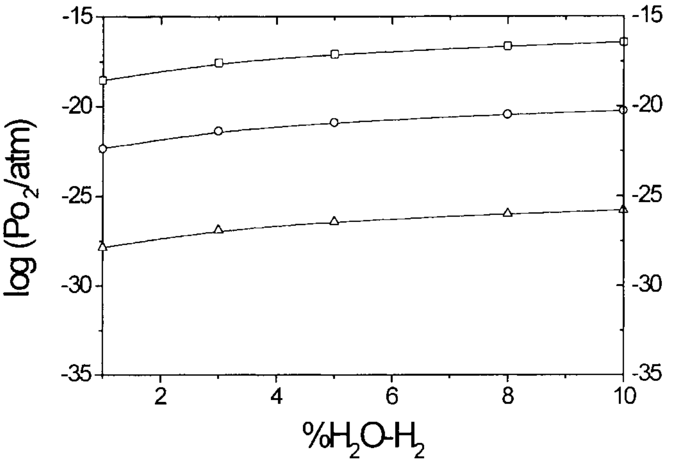

Fig. 2. Variation of P_{O_2} with H_2O percentage in the mixted fuel gas of H_2O–H_2 at different temperatures. (For the meaning of %H_2O–H_2 see text.) Key: (△) 600; (○) 800 and (□) 1000 °C.

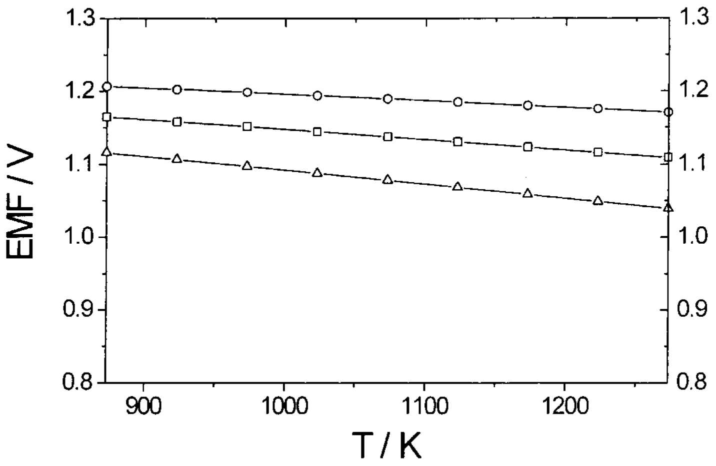

Fig. 3. Characteristics of the e.m.f. as a function of temperature for the cell [I] of P''_{O_2}, Pt (anode)| electrolyte |Pt (cathode), $P'_{O_2} = 1$ atm. Key: (○) 1%H_2O–H_2; (□) 3%H_2O–H_2; (△) 10%H_2O–H_2.

H_2O percentage of H_2O–H_2, as shown in Figure 3, the e.m.f.'s all fall with increasing temperature. For example, when the anode is fed with 3%H_2O–H_2, which can be achieved by bubbling H_2 through water at about 25 °C, the e.m.f.'s decrease from 1.16 V at 600 °C to 1.11 V at 1000 °C.

3.2. $P^*_{O_2}$ *effect on e.m.f.*

To a mixed conduction electrolyte, the characteristic oxygen partial pressure $P^*_{O_2}$ has a significant impact on the e.m.f. according to Equation 20. From this equation the theoretically calculated e.m.f.'s of cell [I] as a function of log $P^*_{O_2}$ are given in Figure 4, assuming the cell operates at 800 °C. Three types of fuel gas of 1%, 3% and 10% H_2O–H_2 were fed to the anode, respectively. The corresponding curves tend to coincide at approximately $P^*_{O_2} = 10^{-15}$ atm. With the decrease in $P^*_{O_2}$, all the curves approach the theoretical e.m.f.'s, that is, 1.19, 1.14 and 1.08 V, of purely ionic electrolyte at approximately $P^*_{O_2} = 10^{-30}$ atm. It is well recognized that $(ZrO_2)_{0.92}(Y_2O_3)_{0.08}$(8YSZ) is usually described as a pure oxygen-ion conductor since its $P^*_{O_2}$ is below 10^{-30} atm at 800 °C [23]. So the cell based on a YSZ electrolyte can be used stably under a reducing atmosphere. Conversely, some mixed conducted electrolytes such as doped CeO_2 are

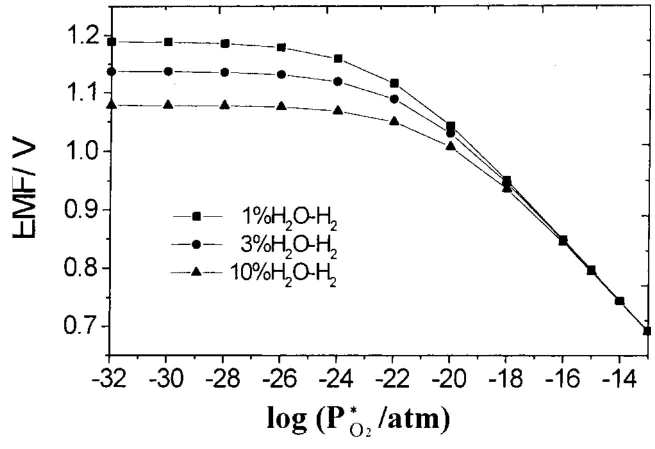

Fig. 4. Calculated e.m.f.'s of the cell [I] as a function of log $P^*_{O_2}$ at 800 °C.

less stable under the reduced anodic atmosphere. The higher $P^*_{O_2}$ gives rise to a lower e.m.f. that may reduce the electrical energy efficiency of a fuel cell, which agrees with a number of experimental results.

The characteristic oxygen partial pressure $P^*_{O_2}$ is an intrinsic property of the electrolyte. The temperature dependence of $P^*_{O_2}$ has been studied for several fluorite structure electrolytes [14, 17, 20]. Tuller and Nowick [17] reported the characteristics of $\log P_{O_2}$ against T^{-1} at some values of t_{ion} for the electrolyte $(CeO_2)_{0.95}(Y_2O_3)_{0.05}$ and the results show a linear relationship. For the case of $t_{ion} = 0.5$, at which $P^*_{O_2}$ is determined, the relation between $P^*_{O_2}$ and T^{-1} can be expressed by the following equation which gives a straight line on an Arrhenius plot:

$$P^*_{O_2}(\mathrm{atm}) = 1.07 \times 10^{17} \exp\left(\frac{-369\,\mathrm{kJ}}{RT\,\mathrm{mol}}\right) \tag{25}$$

A similar equation can be also obtained for the electrolyte $(CeO_2)_{0.9}(Gd_2O_3)_{0.1}$ from the experimental results by Kudo and Obayashi [14] as follows:

$$P^*_{O_2}(\mathrm{atm}) = 1.25 \times 10^{12} \exp\left(\frac{-578\,\mathrm{kJ}}{RT\,\mathrm{mol}}\right) \tag{26}$$

Log $P^*_{O_2}$ against $1000/T$ is plotted as Figure 5 for the above electrolyte. It can be seen that a mixed conductor has a higher $P^*_{O_2}$ at elevated temperatures. The combined influence of $P^*_{O_2}$ and temperature on the e.m.f.'s is also shown in Figure 5 when the fuel gas is 3% H_2O–H_2. It is found that the e.m.f. decreases with increasing temperature.

To enhance e.m.f.'s of the fuel cells based on a mixed conductor much work has been reported [13, 19, 24–26]. One method [13] is to mask the mixed conductor by coating a thin layer ($1 \sim 2$ μm) of stabilized zirconia, which is stable under SOFC operating conditions as discussed above. It is shown that, by coating a thin layer of zirconia, the interface partial pressure of oxygen can be maintained high enough to prevent the electrolyte from reduction. Another effective method is to increase the characteristic oxygen partial pressure of the electrolyte in appropriate ways. One example is that of Maricle et al. [24] on $Ce_{0.8}Gd_{0.2}O_{1.9}$ who doubly doped Pr in gadolina-doped ceria. Sammes and Cai [19] also investigated this electrolyte with addition of $1 \sim 5$ mol % YSZ and found that the $P^*_{O_2}$ can decrease from 10^{-15} atm to 10^{-17} atm, showing greater stability of the system containing YSZ.

3.3. *Anodic P''_{O_2} effect on e.m.f.*

According to Equation 20, the oxygen partial pressure, P''_{O_2}, at the anode is also a factor which influences the e.m.f. Figure 6 shows the relation between the e.m.f. and the oxygen partial pressure at the anode at 800 °C, provided the cathode is operated at 1 atm oxygen gas. When the anodic oxygen partial pressures increase from 4.5×10^{-23} atm (1% H_2O–H_2) to 5.5×10^{-21} atm (10% H_2O–H_2), the e.m.f.'s decrease by 0.11 V (from 1.19 to 1.08 V) for the fuel cell based on a purely ionic electrolyte. At the same time, the e.m.f.'s decrease less with increasing $P^*_{O_2}$ than the purely ionic oxide. For example, the e.m.f.'s decrease only by 0.03 V (from 0.797 to 0.794 V) for the fuel cell based on a mixed conducting oxide with $P^*_{O_2} = 10^{-15}$ atm. It is likely that concentration polarization at the anode has a less detrimental effect on the e.m.f. of a mixed conduction electrolyte-based SOFC than of a purely ionic electrolyte-based SOFC.

On the one hand, for the fuel cell based on a purely ionic electrolyte, it can be derived from Equation 22 that the e.m.f. will become significantly high when P''_{O_2} becomes very low. On the other hand, for the fuel cell based on a mixed conduction electrolyte, from Equation 20, the e.m.f. becomes larger as P''_{O_2} reduces until it reaches a maximum value as

$$E = \frac{RT}{4F}\ln\left(\frac{P'_{O_2}}{P^*_{O_2}}\right) \tag{27}$$

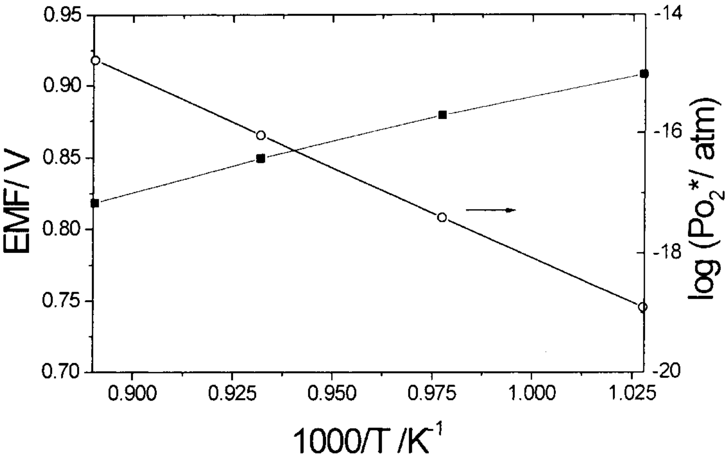

Fig. 5. Variation of $P^*_{O_2}$ with reciprocal absolute temperature for $Ce_{0.8}Gd_{0.2}O_{1.9}$. Combined influence of $P^*_{O_2}$ and temperature on e.m.f.'s is also shown when the fuel gas is 3%H_2O–H_2.

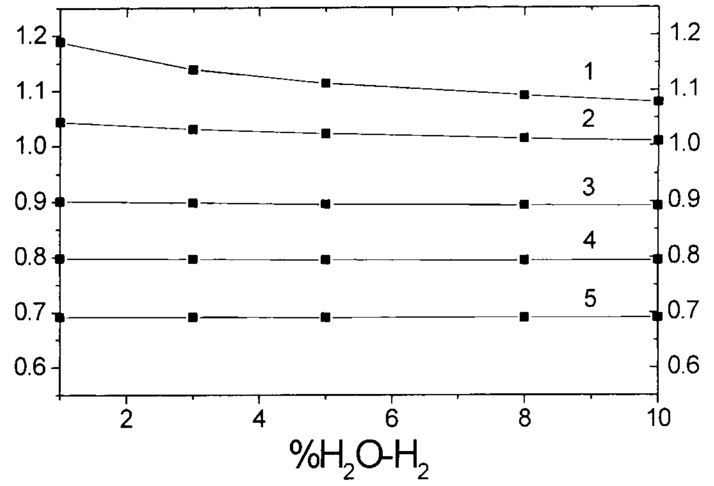

Fig. 6. E.m.f. as a function of P''_{O_2} (%H_2O–H_2) at the anode for a purely ionic electrolyte and different $P^*_{O_2}$ mixed conductor-based fuel cells working at 800 °C (curves 1–5 represent electrolytes of purely ionic oxide and those with log $P^*_{O_2}$(atm) $= -20, -17, -15, -13$).

at which $P''_{O_2} \ll P^*_{O_2} \ll P'_{O_2}$. For example, when $P'_{O_2} = 1$ atm and $P''_{O_2} \ll P^*_{O_2}$, the maximum e.m.f.'s at 800 °C are 0.692, 0.798 and 0.958 V for the cells whose $P^*_{O_2} = 10^{-13}$, 10^{-15} and 10^{-18} atm, respectively. Therefore, for this kind of fuel cell, the effect of reducing the oxygen partial pressure of the fuel gas at the anode is limited in order to enhance the e.m.f. More effective methods rely on the adoption of appropriate electrolytes with higher $P^*_{O_2}$ or the improvement of their ionic domains, which have been discussed in Section 3.2.

4. Conclusions

We have theoretically calculated the electromotive force of SOFCs based on fluorite structured electrolyte. Several calculation equations are deduced based on defect chemistry analysis. To a purely ionic electrolyte-based fuel cell, the e.m.f. decreases with increasing operation temperature when the anode is fed with a certain H_2O–H_2 gas mixture. The characteristic oxygen partial pressure $P^*_{O_2}$ (at which the ionic transference number of the electrolyte is 1/2) has a significant impact on the e.m.f. A higher $P^*_{O_2}$ gives rise to a lower e.m.f. that will reduce the energy conversion efficiency, which is often seen in a mixed conduction electrolyte-based fuel cell. Many methods can be taken to enhance the e.m.f. of a fuel cell based on a mixed conductor. It is also concluded that the low anodic oxygen partial pressure has a much smaller influence on the fuel cell based on mixed conduction electrolyte than on that based on a pure ionic electrolyte.

Acknowledgements

Grant numbers, 29631020 and 29801003, from the National Science Foundation of China, made this publication possible.

References

1. N.Q. Minh, *J. Am. Ceram. Soc.* **76** (1993) 563.
2. E.P. Murray, T. Tsai and S.A. Barnett, *Nature* **400** (1999) 649.
3. G. Meng, W. Liu and D. Peng, *Ionics* **4** (1998) 451.
4. A.M. Azad, S. Larose and S.A. Akbar, *J. Mater. Sci.* **29** (1994) 4135.
5. T. Ishihara, M. Honda, T. Shibayama, H. Nishiguchi and Y. Takita, *J. Electrochem. Soc.* **145** (1998) 3177.
6. K. Huang, R.S. Tichy and J.B. Goodenough, *J. Am. Ceram. Soc.* **81** (1998) 2581.
7. N. Bananos, B. Ellis and M.N. Mahmood, *Solid State Ionics* **144** (1991) 305.
8. H. Iwahara, T. Yajima, T. Hibino and H. Ushida, *J. Electrochem. Soc.* **140** (1993) 1687.
9. B. Zhu and B.-E. Mellander, *J. Power Sources* **52** (1994) 289.
10. S. Tao, Q. Wu, D. Peng and G. Meng, *J. Appl. Electrochem.* **30** (2000) 2.
11. C. Wagner, *Z. Phys. Chem.* **B41** (1933) 42.
12. H. Rickert, 'Electrochemistry of Solids – An Introduction' (Springer, Berlin, Heidelberg, 1982), p. 99.
13. A.V. Virkar, *J. Electrochem. Soc.* **138** (1991) 1481.
14. T. Kudo and H. Obayashi, *J. Electrochem. Soc.* **123** (1976) 415.
15. D.S. Tannhauser, *J. Electrochem. Soc.* **125** (1978) 1277.
16. N.Q. Minh and T. Takahashi, 'Science and Technology of Ceramic Fuel Cells' (Elsevier Science B.V., Amsterdam, 1994), p. 50.
17. H.L. Tuller and A.S. Nowick, *J. Electrochem. Soc.* **122** (1975) 255.
18. H. Arai, T. Kunisaki, Y. Shimizu and T. Seiyama, *Solid State Ionics* **20** (1986) 241.
19. N.M. Sammes and Z. Cai, *Solid State Ionics* **100** (1997) 39.
20. T. Takahashi, T. Esaka and H. Iwahara, *J. Appl. Electrochem.* **7** (1977) 303.
21. H.J.M. Bouwmeester, H. Kruidhof, A.J. Burggraaf and P.J. Gellings, *Solid State Ionics* **53–56** (1992) 460.
22. J.W. Patterson, E.C. Bogren and R.A. Rapp, *J. Electrochem. Soc.* **144** (1967) 752.
23. H. Schmalzried, *Z. Elektrochem.* **66** (1962) 572.
24. D.L. Maricle, T.E. Swarr and S. Karavolis, *Solid State Ionics* **52** (1992) 173.
25. T. Tai, E.P. Murray and S.A. Barnett, *J. Electrochem. Soc.* **144** (1997) L130.
26. Y. Mishima, H. Mitsuyasu, M. Ohtaki and K. Eguchi, *J. Electrochem. Soc.* **145** (1998) 1004.